Building Adaptive Multiresolution Schemes within Harten's Framework

Francesc Aràndiga and Rosa Donat

Abstract. We consider the cell-average framework described by A. Harten in [5], and build the prediction operator using two nonlinear interpolation techniques. We test the resulting nonlinear, adaptive, multiresolution scheme, and compare it with a linear scheme of the same accuracy. The nonlinear prediction processes we develop can also be used in the context of iterative refinement. Numerical tests show that this is also a viable alternative for piecewise smooth data.

§1. Introduction

The goal of a multi-scale decomposition of a discrete set of data is a "rearrangement" of its information content in such a way that the new discrete representation, exactly equivalent to the old one, is more "manageable" in some respects. Some of the best known applications of multi-scale decompositions derive from their compression capabilities: a multiresolution representation of a function, i.e., of a discrete set which represents the function in some sense, can be highly compressed with minimal loss of information content. Precisely because of this potential, multi-scale techniques have an emergent role in numerical analysis, where the multi-scale idea has been used successfully over the years, from multigrid techniques to hierarchical bases in finite element spaces or subdivision schemes in Computer-Aided Design (CAD).

In the late 80's and early 90's, ideas from all these fields, together with a wide experience in the numerical solution of Hyperbolic Conservation Laws (HCL) lead Ami Harten to develop a *General Framework* for multiresolution representation of discrete data. The building blocks of a multiresolution scheme *à la Harten* are two operators which connect discrete and continuous data: The *discretization operator* obtains discrete information from a given signal (belonging to a particular function space) at a given resolution level; the *reconstruction operator* produces an approximation to that signal (in the same function space) from its discretized values.

Curve and Surface Fitting: Saint-Malo 1999
Albert Cohen, Christophe Rabut, and Larry L. Schumaker (eds.), pp. 19–26.

ISBN 0-8265-1357-3.

Harten's point of view is that the way in which the discrete data is generated, i.e., the discretization process, determines its *nature* and should provide an adequate setting for a multiresolution analysis. Once the setting is specified, the choice of an appropriate reconstruction operator provides the key step to the construction of a multiresolution scheme.

The reconstruction process lies at the very heart of a multiresolution scheme built *à la Harten*, and adaptivity can be introduced in the multiresolution scheme at this level. A nonlinear, adaptive reconstruction technique which fits the approximation to the local nature of the data will lead to a nonlinear adaptive multiresolution algorithm with improved compression capabilities.

The aim of this study is to examine a particular class of nonlinear adaptive multiresolution schemes, those using the Essentially Non Oscillatory (ENO) interpolatory techniques of [6] in the reconstruction step. Numerical experiments [1,2] show that ENO-MR schemes have larger compression rates than linear ones when the original signal or image is composed of smooth parts joined together by singularities. ENO techniques can be used to construct very accurate interpolants, which in turn lead to multiresolution schemes with high compression capabilities. When the original signal is geometric, nonlinear schemes can be used as loss-less compression techniques, and we show some application of this in the last section of this paper.

The nonlinear prediction process can be used also in the context of subdivision refinement. This amounts to setting to zero all scale coefficients and using the prediction operator to proceed by dyadic refinement. Preliminary tests show that these nonlinear subdivision schemes lead to non-oscillatory limiting functions when applied to piecewise smooth data with jumps, and open up an interesting alternative for iterative refinement of piecewise smooth data.

§2. Cell Average Multiresolution Analysis

When dealing with discrete data coming from a piecewise smooth function, the simplest discretization process, that of considering the *point-values* of the function, might not be well defined, especially at jump discontinuities. On the other hand, the discretization by cell-averages procedure acts naturally on the space of integrable functions, and it provides a more adequate setting to deal with piecewise smooth signals. Because of this, we shall carry out our numerical study within the cell-average framework.

Images are considered here as two-dimensional signals, and we use the usual tensor-product approach to design our two-dimensional algorithms. Thus, we only describe the essential features of the one-dimensional setting for the sake of completeness. The interested reader can find the missing details in this section in [2] or [5].

Let us consider a set of nested dyadic grids in [0,1]:

$$X^k = \{x_i^k\}_{i=0}^{N_k}, \quad x_i^k = ih_k, \quad h_k = 2^{-k}/N_0, \quad N_k = 2^k N_0, \quad k = L, \ldots, 0,$$

where N_0 is some integer. The discretization by cell average operator is defined as follows:

$$\mathcal{D}_k : L^1[0,1] \longrightarrow V^k, \quad \bar{f}_i^k = (\mathcal{D}_k f)_i = \frac{1}{h_k} \int_{x_{i-1}^k}^{x_i^k} f(x)dx, \quad 1 \le i \le N_k, \quad (1)$$

where $L^1[0,1]$ is the space of absolutely integrable functions in $[0,1]$ and V^k is the space of sequences with N_k components.

Due to the relation

$$\bar{f}_i^{k-1} = \frac{1}{h_{k-1}} \int_{x_{i-1}^{k-1}}^{x_i^{k-1}} f(x)dx = \frac{1}{2h_k} \int_{x_{2i-2}^k}^{x_{2i}^k} f(x)dx = \frac{1}{2}(\bar{f}_{2i-1}^k + \bar{f}_{2i}^k),$$

it is easy to see that $\{\bar{f}_i^k\}_{i=1}^{N_k}$, $k = L-1, \ldots, 0$, can be evaluated directly from $\{\bar{f}_i^L\}_{i=1}^{N_L}$ without using explicitly (1) (i.e., without knowledge of the original function $f(x)$).

To define an appropriate reconstruction operator for this setting (in fact, a whole family of them), we consider the sequence $\{F_i^k\}$ on the k-th grid defined from the cell values $\{\bar{f}_i^k\}$ as follows:

$$F_i^k = h_k \sum_{s=1}^{i} \bar{f}_s^k = \int_0^{x_i^k} f(x)dx = F(x_i^k) \quad \Rightarrow \quad \bar{f}_i^k = \frac{F_i^k - F_{i-1}^k}{h_k}. \quad (2)$$

The function $F(x)$ ($\in C[0,1]$) is, in fact, a primitive of the original function $f(x)$, and the sequence $\{F_i^k\}$ represents a point value discretization of $F(x)$ on the k-th grid (with $F_0^k = 0$). Notice that (2) establishes a one-to-one correspondence between $\{\bar{f}_i^k\}_{i=0}^{N_k}$ and $\{F_i^k\}_{i=0}^{N_k}$.

Let us denote by $\mathcal{I}(x; F^{k-1})$ an interpolatory reconstruction of the set $\{F^{k-1}\}$ on the grid X^{k-1}, i.e., $\mathcal{I}(x_i^{k-1}; F^{k-1}) = F_i^{k-1}$. Then, we obtain an approximation , $\tilde{f}_i^k$, to $\bar{f}_i^k$ using (2) as follows:

$$\tilde{f}_i^k = (\mathcal{I}(x_i^k, F^{k-1}) - \mathcal{I}(x_{i-1}^k, F^{k-1}))/h_k. \quad (3)$$

Since $F_{2i}^k = F(x_{2i}^k) = F(x_i^{k-1}) = F_i^{k-1}$, we obtain

$$\tilde{f}_{2i-1}^k = \frac{1}{h_k}(\mathcal{I}(x_{2i-1}^k, F^{k-1}) - F_{i-1}^{k-1}) \quad \textit{and} \quad \tilde{f}_{2i}^k = \frac{1}{h_k}(F_i^{k-1} - \mathcal{I}(x_{2i-1}^k, F^{k-1})). \quad (4)$$

Let us define the prediction errors as $e_i^k := \bar{f}_i^k - \tilde{f}_i^k$. Using (2) and (4), we easily obtain

$$\bar{f}_{2i-1}^k - \tilde{f}_{2i-1}^k = -(\bar{f}_{2i}^k - \tilde{f}_{2i}^k).$$

Thus, we can simply store only the prediction errors with odd indexes; these are the scale coefficients, $d_i^k = e_{2i-1}^k$, of the multiresolution transform.

The multiscale decomposition of the original data $\bar{f}^L$ is described by the encoding algorithm:

$$\begin{cases} Do & k = L, \ldots, 1 \\ & \bar{f}_i^{k-1} = \frac{1}{2}(\bar{f}_{2i-1}^k + \bar{f}_{2i}^k) \qquad 1 \le i \le N_{k-1} \\ & d_i^k = \bar{f}_{2i-1}^k - (\mathcal{I}(x_{2i-1}^k; F^{k-1}) - F_{i-1}^{k-1})/h_k \quad 1 \le i \le N_{k-1}. \end{cases} \tag{5}$$

We recover the original data with the decoding algorithm:

$$\begin{cases} Do & k = 1, \ldots, L \\ & \bar{f}_{2i-1}^k = (\mathcal{I}(x_{2i-1}^k; F^{k-1}) - F_{i-1}^{k-1})/h_k + d_i^k \qquad 1 \le i \le N_{k-1} \\ & \bar{f}_{2i}^k = 2\bar{f}_i^{k-1} - \bar{f}_{2i-1}^k \qquad 1 \le i \le N_{k-1}. \end{cases} \tag{6}$$

In our study we consider only local interpolation techniques with Lagrangian polynomials, i.e.,

$$\mathcal{I}(x; F^k) = q_i(x; F^k) \qquad x \in [x_{i-1}^k, x_i^k],$$

where $q_i(x; F^k)$ is a polynomial of degree r satisfying $q_i(x_{i-1}^k; F^k) = F_{i-1}^k$ and $q_i(x_i^k; F^k) = F_i^k$.

When the stencil of points used to construct $q_i(x)$ is symmetric around the ith interval (i.e., $r = 2s-1$, $\mathcal{S} = \{x_{i-s}^k, \cdots, x_{i+s-1}^k\}$), we obtain a centered interpolation technique. Centered interpolation techniques are very often used in approximation theory because they minimize the interpolation error, thus leading to very accurate reconstructions of smooth signals. It turns out that the multiresolution schemes obtained from (5) and (6) with Lagrangian piecewise polynomial centered interpolation techniques are equivalent to the Biorthogonal Wavelet (BOW) schemes of [4] (with the box function as the scaling function).

The compression properties of BOW schemes have been widely analyzed in the literature, but from an approximation theory standpoint, it is very easy to study the behavior of the coefficients in terms of the smoothness of the underlying signal and the accuracy of the interpolation technique. Notice that the scale coefficients d_i^k are related to interpolation errors at the odd points of the k-th grid. In fact,

$$d_i^k = (F_{2i-1}^k - \mathcal{I}(x_{2i-1}^k; F^{k-1}))/h_k.$$

Thus, if $f(x)$ is sufficiently smooth at $[x_{i-1}^{k-1}, x_i^{k-1}]$, we have $d_i^k = O(h_{k-1}^r)$. However, the presence of an isolated singularity $x_d \in [x_{i-1}^{k-1}, x_i^{k-1}]$ induces a loss of accuracy in the polynomial pieces whose stencils cross the singularity. The accuracy loss is related to the strength of the singularity as follows [2]: if $[f^{(p)}]_{x_d} = f^{(p)}(x_d+) - f^{(p)}(x_d+) = O(1)$ $(p \le r)$, and f is smooth everywhere else, we have

$$d_l^k = \begin{cases} O([f^{(p)}])h_{k-1}^p, & l = i-s, \ldots, i+s-1, \\ O(h_{k-1}^r), & \text{otherwise.} \end{cases} \tag{7}$$

Thus, centered interpolation techniques lead to relatively large regions of poor accuracy around singularities, and therefore to large detail coefficients at those locations where the accuracy loss takes place. The consequence is a loss in efficiency for the multiresolution-based compression scheme.

It seems reasonable to improve the efficiency of the multiresolution-based compression scheme by improving the accuracy of the interpolatory technique used in the reconstruction step. Notice that when the convex hull of the stencil used to construct a polynomial interpolant is contained within a region of smoothness of the underlying signal, the interpolation error (and the corresponding detail coefficient) becomes small. Thus, it is clear that the key point is the construction of polynomial pieces that *avoid the singularity.*

In the literature related to the numerical solution of conservation laws, where discontinuities can spontaneously develop, we find an interpolation procedure with all the features we need: Essentially Non Oscillatory (ENO) interpolatory techniques [6] (it is not surprising that Harten was one of the developers of these techniques).

ENO interpolatory techniques lead to piecewise polynomial interpolants that are fully accurate except in those intervals that contain singularities. The essential feature of ENO interpolatory techniques is a stencil selection procedure that attempts to choose each stencil $\mathcal{S}_i$ within the same region of smoothness of $F(x)$. The stencil selection process uses the divided differences of the discrete set to be interpolated as smoothness indicators: Large divided differences indicate a possible loss of smoothness. The selection process is such that it tends to *look away* from large gradients, when this is feasible.

ENO interpolatory techniques are nonlinear, because the stencil used to construct each polynomial piece depends on the function being interpolated. When the singularities are sufficiently well separated (this means that there are at least $r+1$ points in each smoothness region), ENO techniques lead to stencils such that (assuming the singularity is located at the ith cell) $\mathcal{S}_{i-1} \cap \mathcal{S}_{i+1} = \emptyset$. Hence, the detail coefficients satisfy

$$d_l^k = \begin{cases} O([f^p])h_{k-1}^p, & l = i, \\ O(h_{k-1}^r), & \text{otherwise.} \end{cases} \tag{8}$$

Thus ENO interpolants have a nearly optimal high accuracy region, which should in turn improve the efficiency of the corresponding multiresolution-based compression algorithms.

The case of a corner of f (i.e., a jump in f') is especially interesting because it is possible to construct an even better (in terms of local accuracy) interpolant: the ENO-SR interpolant.

The Subcell Resolution (SR) technique (also due originally to Harten [3]) allows us to obtain an approximation to the *location* of an isolated corner in a continuous function up to the order of the truncation error. The approximated value is then used to modify locally (in the interval where the discontinuity lies) the definition of the piecewise polynomial interpolant in such a way that the interpolation error is small except for an $O(h^{r+1})$ band around the corner.

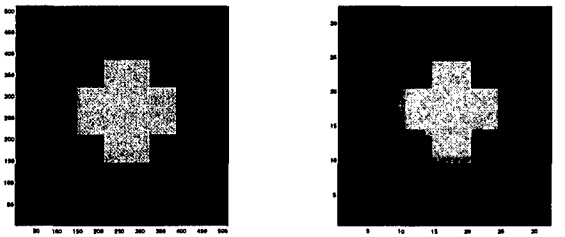

Fig. 1. Left original, right coarse version.

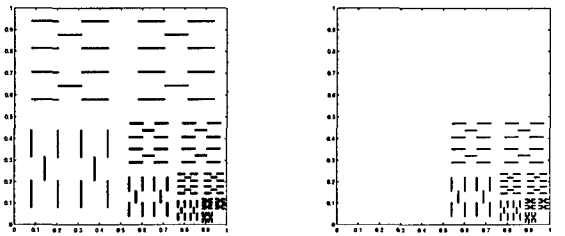

Fig. 2. Left linear, right ENO.

Recall that in the cell-average setting, the interpolation process is applied to the primitive function. Since jumps in $f(x)$ become corners in $F(x)$, using an ENO-SR interpolant in the reconstruction step lead to detail coefficients satisfying

$$d_l^k = O(h_{k-1}^r), \quad \text{except when} \quad x_{2l-1}^k \approx x_d. \tag{9}$$

The SR technique is, thus, appropriate to increase the efficiency of multiresolution-based compression algorithm for piecewise continuous functions with jumps.

§3. Numerical Experiments

Let us consider a purely geometric image as shown in Figure 1 (left), and apply to it the tensor-product version of algorithm (5). We consider piecewise polynomial interpolants of degree 4, thus the accuracy of the reconstruction in the cell-average framework is 3. In Figure 2 we display the location of non-zero scale coefficients in the multiresolution representation of the signal. When using the ENO-SR technique, and because all discontinuities are "aligned with the (tensor-product) grid", all scale coefficients are zero. This is a direct consequence of the fact that the ENO-SR reconstruction commits no error at the odd points in each one of the resolution levels considered ($L = 4$ in this example). In the case of the ENO scheme, the scale coefficients at the highest resolution level are all zero. This is a consequence of the nature of the data (the point-values of the signal at the highest resolution level), which locates all discontinuities at the cell end-points. The ENO technique is perfectly

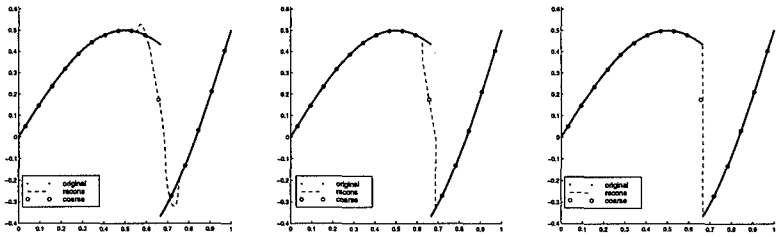

Fig. 3. 1d Linear, ENO, ENO-SR.

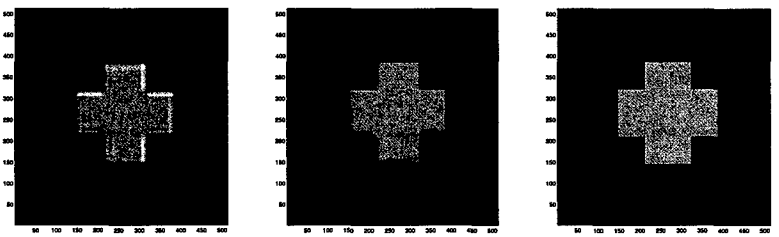

Fig. 4. Reconstruction from the coarse: linear, ENO, ENO-SR.

accurate when the discontinuity is located at a grid point. The technique is fully accurate at all the lower resolution levels except at the interval where the discontinuity is located. Thus, there is only one scale coefficient, located at the point which is closest to the singularity. This should be compared with the 3 scale coefficients per singularity obtained with the linear scheme (the lines showing the location of non-zero scale coefficients are thicker for the linear scheme). For the sake of comparison, the number of non-zero scale coefficients in each case is: Linear 8554, ENO 1688, ENO-SR 0.

We turn next to the nonlinear subdivision scheme obtained by considering the ENO and ENO-SR in the prediction process. In Figure 3 we show a univariate process. Starting from the the cell-averages of a piecewise smooth function at a very coarse level (16 points), we proceed by dyadic refinement until we obtain 1024 data. The numerical results clearly indicate that no overshoots or undershoots are obtained with the non-linear techniques. Again, the excellent properties of the ENO-SR technique in terms of approximation lead to the best results.

In Figure 4 we show a simple multivariate test, the reconstruction of the geometric figure considered before from a very coarse representation (right in Figure 1). The Gibbs-like oscillations typical of linear schemes in the presence of discontinuities lead to the blurring of the edges observed in Figure 4 (left). There is no blurring in the reconstructed image obtained with the nonlinear techniques. Again, the ENO-SR scheme leads, in this simple case, to the exact original image. One dimensional cuts of the reconstructed figures are displayed in Figure 5.

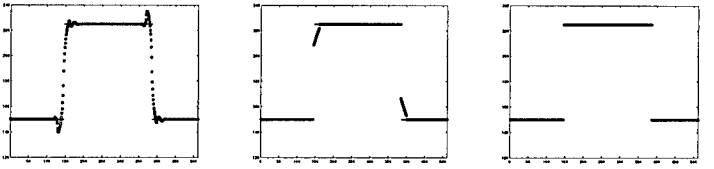

Fig. 5. Horizontal cuts linear, ENO, ENO-SR.

Acknowledgments. Supported in part by DGICYT PB97-1402 and in part by TMR project ERBFMRX-CT98-0184.

References

1. Amat, S., F. Aràndiga, A. Cohen, and R. Donat, Tensor product multiresolution analysis with error control, Technical Report GrAN-99-4, University of València, 1999.
2. Aràndiga, F., and R. Donat, A class of nonlinear multiscale decompositions, Technical Report GrAN-99-1, University of València, 1999. (Also submitted to Numerical Algorithms).
3. Harten, A., ENO schemes with subcell resolution, J. Comput. Phys. **83** (1989), 148–184.
4. Cohen, A., I. Daubechies, and J. C. Feauveau, Biorthogonal bases of compactly supported wavelets, Comm. Pure Applied Math. **45** (1992), 485–560.
5. Harten, A., Multiresolution representation of data II: General framework, SIAM J. Numer. Anal. **33** (1996), 1205–1256.
6. Harten, A., B. Engquist, S. Osher, and S. Chakravarthy, Uniformly high order accurate essentially non-oscillatory schemes III, J. Comput. Phys. **7** (1987), 231–303.

F. Aràndiga and R. Donat
Departament de Matemàtica Aplicada.
Universitat de València.
4610 Burjassot. València (Spain)
donat@uv.es
arandiga@uv.es